Reduction of CuO in H_2: *in situ* time-resolved XRD studies

José A. Rodriguez [a,*], Jae Y. Kim [a], Jonathan C. Hanson [a], Manuel Pérez [b], and Anatoly I. Frenkel [c]

[a] Chemistry Department, Brookhaven National Laboratory, Upton, NY 11973, USA
[b] Facultad de Ciencias, Universidad Central de Venezuela, Caracas 1020-A, Venezuela
[c] Department of Physics, Yeshiva University, New York, NY 10016, USA

CuO is used as a catalyst or catalyst precursor in many chemical reactions that involve hydrogen as a reactant or product. A systematic study of the reaction of H_2 with pure powders and films of CuO was carried out using *in situ* time-resolved X-ray diffraction (XRD) and surface science techniques. Oxide reduction was observed at atmospheric H_2 pressures and elevated temperatures (150–300 °C), but only after an induction period. High temperature or H_2 pressure and a large concentration of defects in the oxide substrate lead to a decrease in the magnitude of the induction time. Under normal process conditions, *in situ* time-resolved XRD shows that Cu^{1+} is not a stable intermediate in the reduction of CuO. Instead of a sequential reduction ($CuO \Rightarrow Cu_4O_3 \Rightarrow Cu_2O \Rightarrow Cu$), a direct $CuO \Rightarrow Cu$ transformation occurs. To facilitate the generation of Cu^{1+} in a catalytic process one can limit the supply of H_2 or mix this molecule with molecules that can act as oxidant agents (O_2, H_2O). The behavior of CuO-based catalysts in the synthesis of methanol and methanol steam reforming is discussed in the light of these results.

KEY WORDS: copper oxide; copper; hydrogen; methanol synthesis; methanol steam reforming; reduction of oxides; X-ray diffraction.

1. Introduction

CuO is used as a catalyst or catalyst precursor in many chemical reactions that involve hydrogen as a reactant or a product: methanol synthesis from CO ($CO + 2H_2 \Rightarrow CH_3OH$) or CO_2 ($CO_2 + 3H_2 \Rightarrow CH_3OH + H_2O$) [1–3], the water–gas shift reaction ($CO + H_2O \Rightarrow CO_2 + H_2$) [4], methanol steam reforming ($CH_3OH + H_2O \Rightarrow CO_2 + 3H_2$) [5], oxidative methanol reforming ($CH_3OH + \frac{1}{4}O_2 + \frac{1}{2}H_2O \Rightarrow CO_2 + \frac{5}{2}H_2$) [6], NO reduction ($NO + H_2 \Rightarrow \frac{1}{2}N_2 + H_2O$) [1,7], etc. It has been proposed that in several of these catalytic processes CuO undergoes a complete reduction and metallic copper or Cu^0 is the real active phase [8–12]. For example, after CuO is exposed to mixtures of CO/H_2, measurements using Auger electron spectroscopy (AES) and X-ray photoelectron spectroscopy (XPS) show a $Cu^{2+} \Rightarrow Cu^0$ transformation [8]. Single-crystal surfaces of metallic copper give reaction rates and kinetic parameters that match those obtained for the water–gas shift reaction on CuO/ZnO catalysts [9,10], suggesting that during reaction an active Cu^0 phase is produced. It was thought that the same was valid for the methanol–steam reforming reaction [11,12], but recent studies using *in situ* X-ray diffraction (XRD) and X-ray absorption spectroscopy (XANES/EXAFS) show Cu^{1+} during the reduction of CuO [13]. Time-resolved XANES also shows Cu^{1+} as a transient species in the reduction of CuO/ZnO catalysts during the oxidative reforming of methanol [14]. For years, there has been a controversy about the relative importance of Cu^{1+} and Cu^0 centers in the methanol synthesis reaction [1–3,10]. In order to solve some of these issues, one needs a fundamental understanding of the reaction of H_2 with CuO and the microscopic mechanism for the reduction of the oxide.

CuO, Cu_4O_3 and Cu_2O are oxides of copper with well-defined crystal structures [15–17]. Thus, a sequential reduction of copper oxide ($CuO \Rightarrow Cu_4O_3 \Rightarrow Cu_2O \Rightarrow Cu$) upon reaction with H_2 could occur. The data reported in the literature do not agree on this point. Experiments of H_2 temperature-programmed reduction (TPR) show that the reduction of CuO occurs in one, two or even three steps [18–20]. XANES points to the existence of Cu^{1+} as a transient species in the reduction of Cu^{2+} to Cu^0 [13,14,21], but such an intermediate was not detected in XRD measurements [22]. These discrepancies could be a consequence of the different conditions used in the reduction experiments, or they could originate from differences in the preparation of the samples with CuO deposited on different supports (Al_2O_3, ZnO, Y-ZrO_2, ZSM-5). Therefore, we decided to perform a systematic study of the reaction of H_2 with pure powders and films of CuO using *in situ* time-resolved XRD and surface science techniques.

It is very important to examine the reduction of CuO with H_2 *in situ*, because for this system *ex situ* investigations may not represent the "real" state of the copper phase under reduction conditions [13,14]. Nowadays the combination of the high intensity of synchrotron radiation with new data collection devices makes it possible to conduct sub-minute, time-resolved XRD experiments under a wide variety of temperature and

pressure conditions ($-190\,°C < T < 900\,°C$; $P < 45\,atm$) [23]. Recently, time-resolved XRD has been successfully used to study the reduction of MoO_3 [24] and NiO [25] *in situ* under atmospheric pressures of H_2.

2. Experimental

2.1. Time-resolved XRD studies

High-purity (99.995%) powders of CuO were acquired from commercial sources. These powders exhibited the typical Cu 2p XPS [8,26], Cu L_3VV Auger [26,27] and O K-edge XANES [28] spectra of pure CuO. The time-resolved XRD data were collected on beam line X7B of the National Synchrotron Light Source (NSLS) [23]. Samples of CuO were loaded in an open sapphire capillary attached to a flow-reaction cell similar to those described previously [29,30]. The capillary was connected to 1/16 in. Swagelok style fittings with Vespel ferrules. A 0.010 in. chromel–alumel thermocouple was inserted straight into the capillary near the oxide sample [29]. The oxide sample was heated using a small resistance heater wrapped around the capillary. Diffraction patterns ($\lambda = 0.9036$ or $0.9201\,\text{Å}$) were recorded at temperatures in the range 150–300 °C under a 5% H_2 (99.9999% purity) and 95% He (99.9999% purity) gas mixture (flow rate ~ 1 or $20\,\text{cm}^3$/min) using a MAR345 detector. The typical time required for collecting an individual diffraction pattern was in the range 1–3 min. The powder rings were integrated using the FIT2D code [31].

2.2. XPS and AES studies

The experiments for the reaction of H_2 with CuO films were performed in a standard ultrahigh-vacuum (UHV) system, base pressure $\sim 2 \times 10^{-10}$ torr, with instrumentation for XPS, AES, low-energy electron diffraction (LEED) and thermal desorption mass spectroscopy (TDS) [25]. The XPS spectra were taken employing Al or MgKα radiation. Attached to the UHV system was a reaction cell [10,25] that was used to expose CuO films to sub-atmospheric pressures of hydrogen. In a typical experiment, the CuO sample was initially cleaned and characterized in the UHV system and subsequently transferred into the reaction cell, where it was exposed to a mixture of H_2 (5 torr, 99.9999% purity) and He (95 torr, 99.9999% purity) at 150–250 °C for a given amount of time. Then, the gases were pumped out and the sample was moved back into the UHV system for surface characterization.

To prepare the CuO films we followed a methodology similar to that described elsewhere [8]. Thick films of metallic copper (99.999% purity) were vapor-deposited on a clean Mo substrate [32]. Then, the metallic Cu was transformed into copper oxide by oxidation with 50 torr of O_2 (5–10 min) at elevated temperatures (400–500 °C) in the reaction cell attached to the UHV chamber [8,26]. These copper oxide films showed the O 1s XPS, Cu 2p XPS and Cu L_3VV Auger spectra expected for CuO [26,27].

3. Results

3.1. Reaction of H_2 with CuO powders

In our experiments with pure powders of CuO, we found reaction with H_2 and reduction to metallic copper at temperatures between 150 and 300 °C. A similar fact has been found in H_2-TPR experiments for the reduction of CuO supported on Al_2O_3 [18] or mixed with ZnO [13]. Figure 1 shows time-resolved XRD data for the isothermal reduction of CuO at 240 °C under a 5% H_2/95% He mixture (gas flow $\sim 20\,\text{cm}^3$/min). These experimental conditions (i.e. temperature, H_2 concentration, flow rate) are similar to those used in many catalytic processes [1,3,10]. In the first 15 min of the experiment, no change is seen in the diffraction pattern for CuO. After this induction time, lines for metallic copper start to appear (direct $Cu^{2+} \Rightarrow Cu^0$ transformation) and the evolution of water is detected at the exit of the reaction cell with a mass spectrometer. This experiment was repeated many times and no diffraction lines for Cu_4O_3 [16] or Cu_2O [17] were seen during the reduction. We also investigated the reduction process at lower temperatures, as shown in figure 2. The decrease in reaction temperature led to an increase in the magnitude of the induction time, but still there was a direct $Cu^{2+} \Rightarrow Cu^0$ transformation without any stable intermediate.

It could be argued that the induction time in figures 1 and 2 is associated with the formation of an amorphous phase of Cu_2O, which may not be detectable with XRD. This possibility was examined using X-ray absorption spectroscopy. Our XANES/EXAFS data indicate that under the experimental conditions of figures 1 and 2 neither Cu_4O_3 nor Cu_2O is formed [33]. In order to see the formation of Cu_2O as a stable intermediate, we had to substantially decrease the flow rate of hydrogen. Figure 3 displays data for the isothermal reduction of CuO powders at 210, 270 and 300 °C under a 5% H_2/95% He mixture and a flow rate of $\sim 1\,\text{cm}^3$/min. In these experiments diffraction lines for Cu_2O (see arrows) clearly appear. The higher the temperature, the larger the amount of Cu^{1+} produced. An analysis of the relative intensities of the diffraction lines indicates that two reduction mechanisms seem to compete and occur simultaneously. These are sequential reduction:

$$2CuO + H_2 \Rightarrow Cu_2O + H_2O \qquad (1a)$$

$$Cu_2O + H_2 \Rightarrow 2Cu + H_2O \qquad (1b)$$
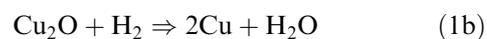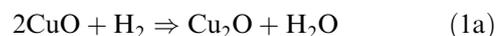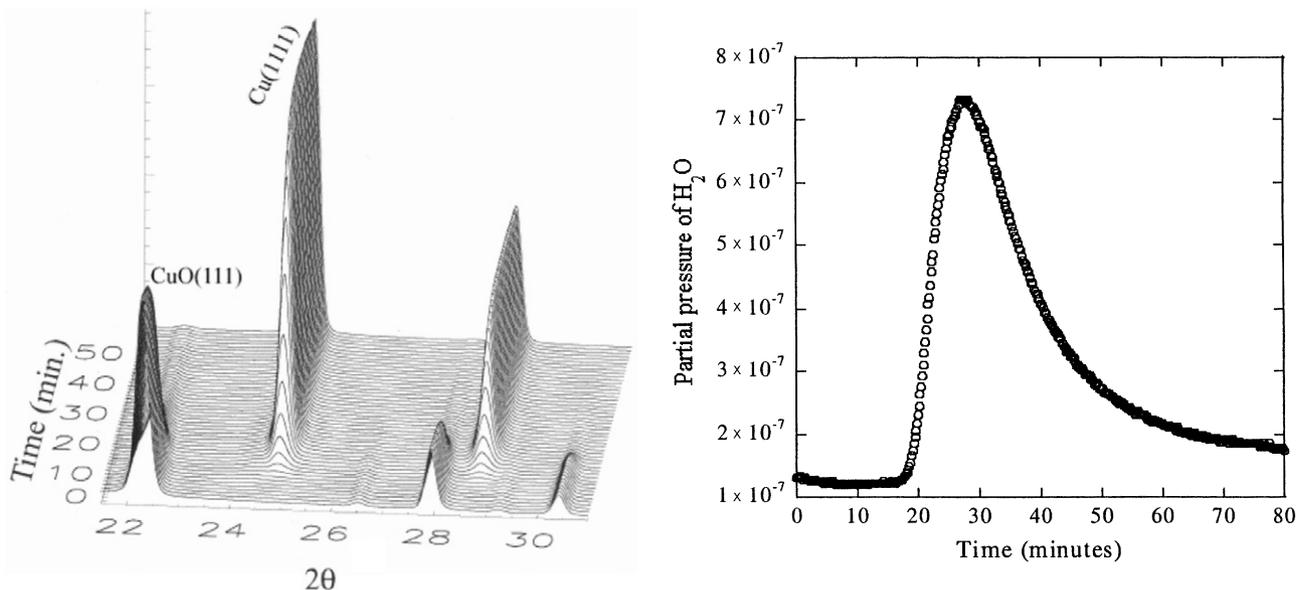
Figure 1. Left: time-resolved XRD data for the reduction of CuO under a 5% H_2/95% He mixture (flow rate $\sim$20 cm^3/min) at 240 °C. Right: evolution of water during the reduction process.

and direct reduction:

$$CuO + H_2 \Rightarrow Cu + H_2O. \qquad (2)$$

Reaction (2) is clearly dominant at 210 and 270 °C, but at 300 °C reaction (1) becomes important. High reaction temperatures and a limited supply of H_2 favor the appearance of Cu^{1+} as an intermediate in the reduction process.

3.2. Reaction of H_2 with CuO films

In agreement with previous studies [8,34], we found that CuO has a very low chemical reactivity under UHV conditions. Figure 4 shows O 1s XPS data for the reduction of CuO films at a temperature of 200 °C with H_2 pressures that range from 10^{-8} to 5 torr. For a very low H_2 pressure of 10^{-8} torr, there is no reaction after 60 min of exposure to the gas. In the case of 10^{-4} torr of H_2, the removal of oxygen from the oxide surface (i.e. drop in O 1s signal) becomes significant after an induction time of $\sim$22 min. Finally, under a H_2 pressure of 5 torr the reduction reaction starts very fast. Thus, high H_2 pressure leads to a decrease in the magnitude of the induction time. The same occurs when defects are introduced in the oxide. For highly defective non-stoichiometric CuO_x films, we found no induction time for reduction under 10^{-4} or 5 torr of H_2 at 200 °C.
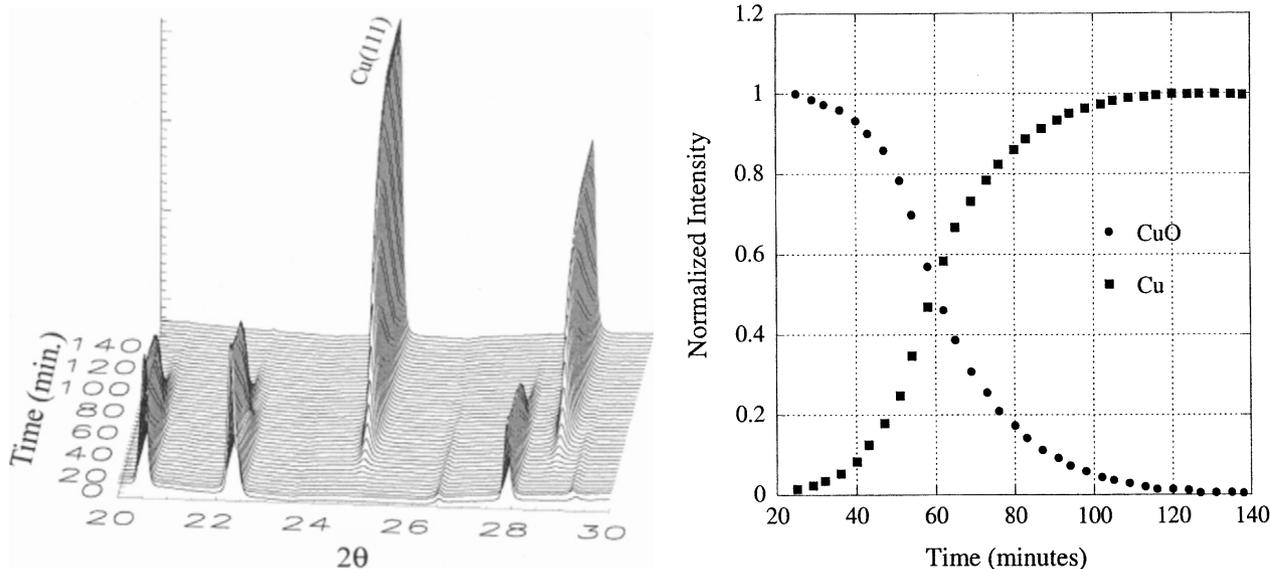
Figure 2. Left: time-resolved XRD data for the reduction of CuO under a 5% H_2/95% He mixture (flow rate $\sim$20 cm^3/min) at 200 °C. Right: amounts of CuO and Cu present as a function of time.
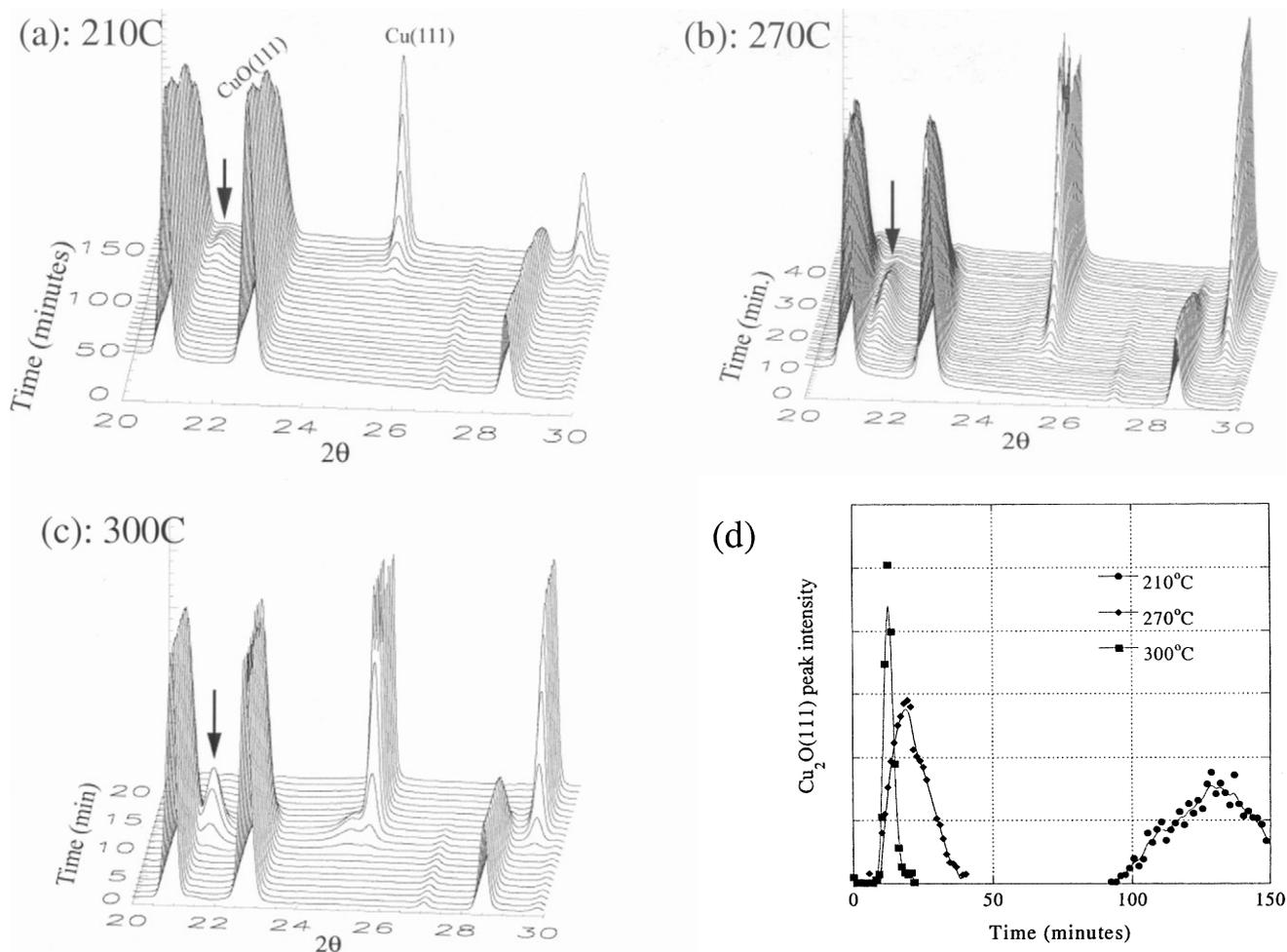
Figure 3. Time-resolved XRD data for the reduction of CuO under a 5% H_2/95% He mixture (flow rate $\sim$1 cm^3/min) at three different temperatures: (a) 210, (b) 270 and (c) 300 °C. The arrows indicate the main diffraction line for Cu_2O. (d) Intensity of the main diffraction line for Cu_2O in each case.

Figure 5 displays Cu 2p and O 1s XPS spectra acquired before and after partial reduction of a CuO film. In the Cu 2p spectrum of CuO strong satellites are observed between 940 and 945 eV [8,26,27]. These satellites are not seen for Cu_2O or metallic Cu [26,27], and are thus a convenient way to monitor the disappearance of CuO during reduction. The Cu L_3VV Auger spectra of CuO, Cu_2O and Cu have distinctive features [26,27], but since they are very broad and close in energy, these Auger spectra have a limited utility when trying to quantify the amount of Cu^{2+}, Cu^{1+} and Cu^0 present in a partially reduced sample of copper oxide. In this respect, the Cu 2p$_{3/2}$ peak position also does not allow a clear distinction of Cu_2O and Cu [26].

As shown in figure 4, the overall rate of reduction is faster under 5 torr of H_2 than under 10^{-4} torr. An important issue here is how the decrease in the CuO Cu 2p satellite signal compares with the decrease in the total O 1s signal. In principle, if a sequential reduction such as reaction (1) occurs, then the CuO satellite signal should drop faster than the O 1s signal. On the

other hand, for a direct reduction like reaction (2), the CuO satellite and O 1s signals should drop in a proportional way. The XPS data in figure 6 show that for a similar drop in the total O 1s signal (i.e. same degree of sample reduction at 10^{-4} and 5 torr), the drop in the CuO satellite signal is larger for the experiment with an H_2 pressure of 10^{-4} torr. These trends point to the existence of a sequential reduction at low H_2 pressure, and a direct reduction at high pressure. This is consistent with the behavior seen above for the reaction of H_2 with CuO powders.

3.3. Reaction of O_2 with CuO_x and Cu

We also investigated the full reoxidation of CuO_x or oxidation of Cu using time-resolved XRD. To compare with the chemistry observed for the reduction of CuO, it is interesting to establish if the oxidation of metallic copper occurs sequentially:

$$2Cu + \tfrac{1}{2}O_2 \Rightarrow Cu_2O \qquad (3a)$$

$$Cu_2O + \tfrac{1}{2}O_2 \Rightarrow 2CuO \qquad (3b)$$
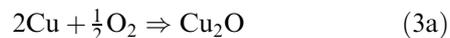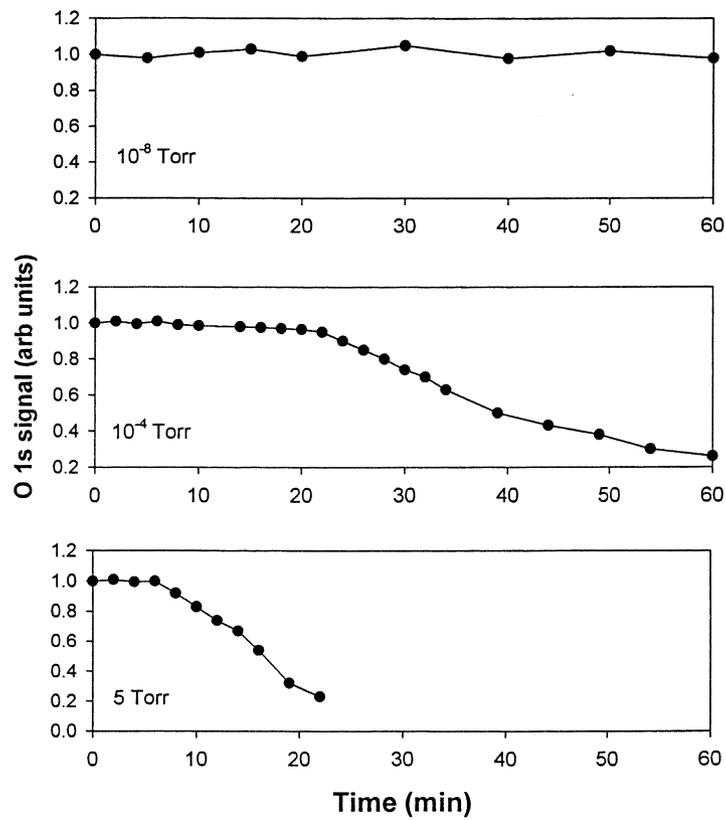
Figure 4. Variation of the O 1s signal as a function of time for the reduction of CuO films at 200 °C under different pressures of H_2.
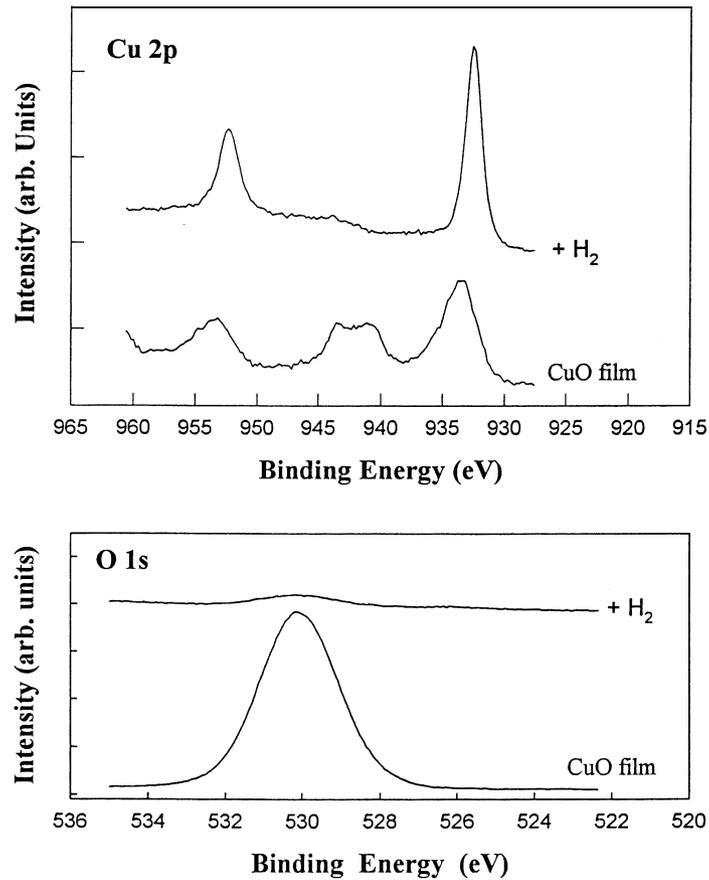
Figure 5. Cu 2p (top panel) and O 1s (bottom panel) XPS spectra taken before and after partial reduction of a CuO film with H_2 at 200 °C.
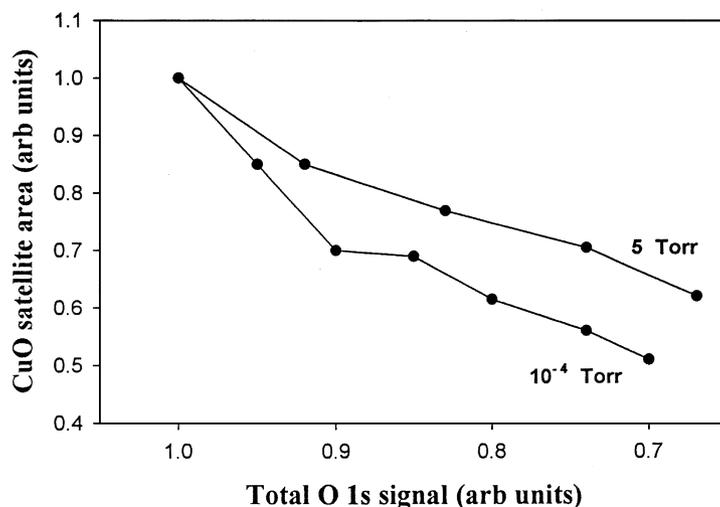
Figure 6. Relationships between the decreases in the CuO Cu 2p satellite area and total O 1s signal for the reduction of CuO under 10^{-4} and 5 torr of H_2.

or through a direct transformation:

$$2Cu + O_2 \Rightarrow 2CuO. \qquad (4)$$

Figure 7 shows time-resolved XRD results for the oxidation of pure Cu in a stream of 5% O_2/95% He (flow rate $\sim$20 cm^3/min) at 300 °C. At this temperature, the full reduction of CuO occurs rapidly under normal conditions (see above). We found that the reverse oxidation of copper is a more difficult process. In figure 7, the diffraction lines for Cu partially disappear, while lines for Cu_2O and a minor amount of CuO appear. After exposing the system for 140 min to O_2, one has a mixture of Cu, Cu_2O (dominant oxide) and CuO.

Complete oxidation of Cu was observed at very high temperatures. Figure 8 displays time-resolved XRD data for the oxidation reaction starting at 30 °C and ending at 600 °C. Here, the lines for metallic Cu decrease in intensity, simultaneously Cu_2O appears, and at the end only CuO is observed at 600 °C.

All our XRD data for the reaction of O_2 with Cu indicate that the oxidation process always follows a sequential pathway as shown in reaction (3). In clear contrast to the behavior observed for the reduction of CuO, Cu^{1+} is a stable intermediate in the oxidation process.

4. Discussion

One method frequently employed for the preparation of active oxide catalysts involves partial reduction with hydrogen at elevated temperatures [1,35]. In general, there is a need to get a fundamental understanding of the reduction/activation process [1,35], and time-resolved XRD can be useful in this respect [24,25,36]. Two different kinetic models have been proposed for the reduction of oxides [1,35]: the "nucleation model" and the "interface-controlled model". In the "nucleation
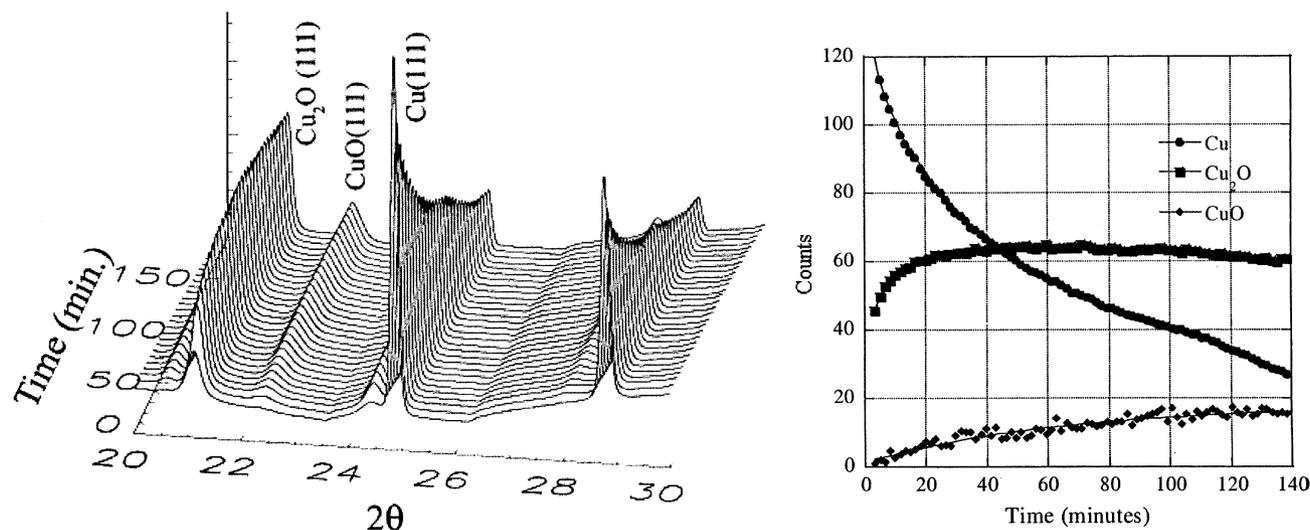
Figure 7. Time-resolved XRD data for the oxidation of Cu under a 5% O_2/95% He mixture (flow rate $\sim$20 cm^3/min) at 300 °C. In the right-hand-side graph is shown the variation of the main diffraction lines for Cu, Cu_2O and CuO as a function of time.
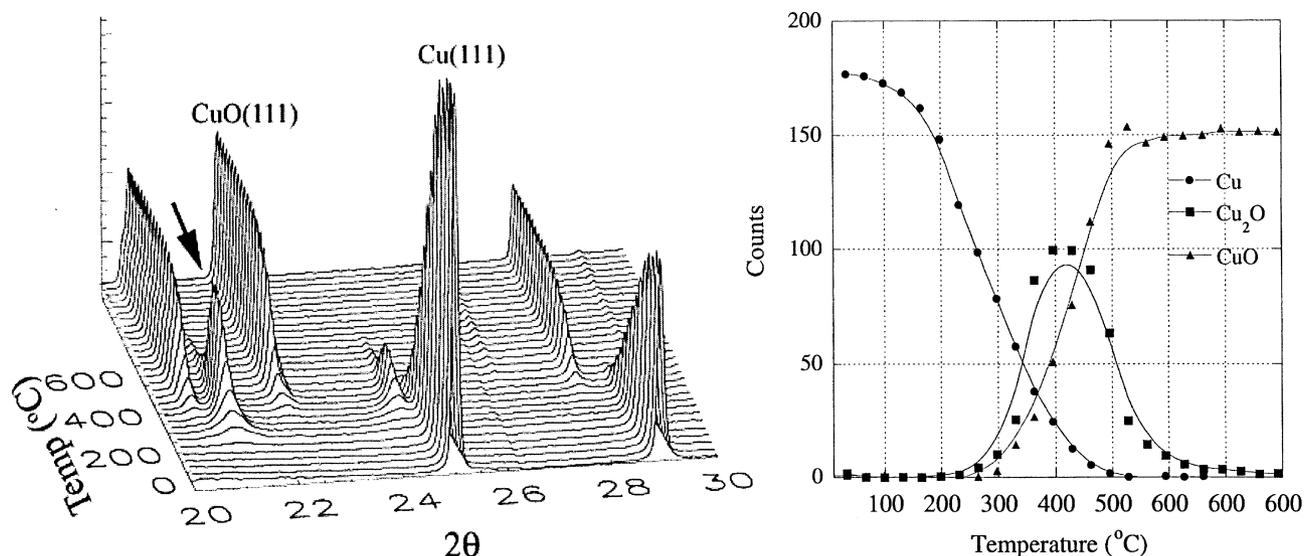
Figure 8. Time-resolved XRD data for the oxidation of Cu under a 5% O_2/95% He mixture (flow rate $\sim$20 cm^3/min) at 25–600 °C and constant 600 °C (30 min). The arrow indicates the main diffraction line for Cu_2O. In the right-hand-side graph is shown the variation of the main diffraction lines for Cu, Cu_2O and CuO as a function of temperature.

(N) model", the generation of small aggregates of active sites for the dissociation of H_2 or clusters of the new phase (i.e. the reduced oxide) is the rate-determining step. According to this model there are two main characteristics in the kinetics for oxide reduction: the existence of an induction period, and the possibility for autocatalysis [1,35]. In the "interface-controlled (IC) model", the rapid formation of a uniform layer of the reduced oxide takes place [35]. A continuous reduced-phase/oxide interface entirely covers the solid reactant, and the rate of oxide reduction is proportional to the area of such interface [35]. In the IC model, the fraction of reduced oxide increases in a non-linear fashion as a function time, without the presence of an induction time or substantial autocatalysis [1,35]. The trends seen in figures 1–4 for the reduction of CuO fit well the nucleation model. The existence of an induction time has also been observed in reduction studies for NiO [25,37,38]. In our experiments with CuO films, we found that the magnitude of the induction time could be reduced substantially by the introduction of defects in the oxide. Thus, the induction time could be associated with the production of sites on the oxide substrate with a high efficiency for the adsorption and dissociation of H_2 [25]. This alone can explain the autocatalytic nature of the reduction process. Once a large coverage of H is available on the surface, then the efficient removal of O from the bulk or the nucleation of the new Cu phase can become rate-limiting factors [35,37].

Under a normal supply of H_2, our results show that Cu^{1+} is not a stable intermediate in the reduction of CuO. It is an open question as to how the system can evolve directly from CuO to Cu without passing through Cu_4O_3 or Cu_2O as intermediates. To address this issue we are currently studying the reduction process using

XANES/EXAFS and diffraction with higher energy ($\lambda \sim 0.15$ Å) X-rays [33]. To faciliate the generation of Cu^{1+} in a catalytic process one can limit the supply of H_2 or mix this molecule with molecules that can act as oxidant agents. We have found that CO also leads to a direct CuO $\Rightarrow$ Cu transformation [39], making difficult the generation of Cu^{1+} during the synthesis of methanol (CO + 2H_2 $\Rightarrow$ CH$_3$OH) on copper oxide-based catalysts. But molecules like H_2O and O_2 can contribute to the generation of Cu^{1+} during methanol steam reforming (CH$_3$OH + H_2O $\Rightarrow$ CO$_2$ + 3H_2) [13] and oxidative methanol reforming (CH$_3$OH + $\frac{1}{4}O_2$ + $\frac{1}{2}H_2O$ $\Rightarrow$ CO$_2$ + $\frac{5}{2}H_2$) [14]. For the reaction of CuO with H_2/O_2/H_2O gas mixtures, time-resolved XRD showed a combination of Cu_2O/Cu as the final product [39]. This is consistent with XANES studies [13,14], which show Cu^{1+} formation during the reforming of methanol over CuO/ZnO catalysts.

Another way to stabilize Cu^{1+} could involve the deposition of CuO on an interacting oxide support. In our H_2-TPR experiments we found desorption of water in a single peak (figure 1), whereas two or even three water desorption peaks have been observed during the reduction of supported CuO [18–20]. Thus, interactions with an oxide support can accelerate or decrease the rate for CuO reduction. It has been proposed that in CuO/ZnO catalysts for the synthesis of methanol, the *intermixing* of the oxides eventually facilitates the formation of Cu^{1+} under reaction conditions [2,3,40]. This requires very strong CuO–ZnO interactions, because both H_2 and CO [39] have a tendency to induce a direct CuO $\Rightarrow$ Cu transformation. The simple deposition of CuO on ZnO is not enough to stabilize Cu^{1+} species and prevent a CuO $\Rightarrow$ Cu conversion [8,39].

5. Conclusions

A systematic study of the reaction of H_2 with pure powders and films of CuO was carried out using *in situ* time-resolved XRD and surface science techniques. At elevated temperatures (150–300 °C), oxide reduction was observed at low (10^{-4} torr) and atmospheric pressures of H_2, but there was an induction period of negligible chemical activity. After the induction period, the reduction process became autocatalytic. A high hydrogen pressure and a large concentration of defects in the oxide substrate led to a decrease in the size of the induction period. The induction period is probably associated with the production (or nucleation) of adsorption sites with a high efficiency for the activation or dissociation of H_2.

Under normal process conditions, *in situ* time-resolved XRD shows that Cu^{1+} is not a stable intermediate in the reduction of CuO. Instead of a sequential reduction ($CuO \Rightarrow Cu_4O_3 \Rightarrow Cu_2O \Rightarrow Cu$), a direct $CuO \Rightarrow Cu$ transformation occurs. To facilitate the generation of Cu^{1+} in a catalytic process one can limit the supply of H_2 or mix this molecule with molecules that can act as oxidant agents (O_2, H_2O).

XRD data for the reaction of O_2 with metallic Cu at 400–600 °C show a sequential oxidation process: $Cu \Rightarrow Cu_2O \Rightarrow CuO$. In clear contrast to the behavior observed for the reduction of CuO, Cu^{1+} is a stable intermediate in the oxidation reaction.

References

[1] H.H. Kung, *Transition Metal Oxides: Surface Chemistry and Catalysis* (Elsevier, New York, 1989).
[2] K. Klier, Adv. Catal. 31 (1982) 243.
[3] J.-L. Li, T. Takeguchi and T. Inui, Appl. Catal. A 139 (1996) 97.
[4] D.S. Newsome, Catal. Rev. Sci. Eng. 21 (1980) 275.
[5] B.A. Peppley, J.C. Amphlett, L.M. Kearns and R.F. Mann, Appl. Catal. A 179 (1999) 31.
[6] T.L. Reitz, P.L. Lee, K.F. Czaplewski, J.C. Lang, K.E. Popp and H. Kung, J. Catal. 199 (2001) 193.
[7] W.-P. Dow and T.-J. Huang, Appl. Catal. A 141 (1996) 17.
[8] C.T. Campbell, K.A. Daube and J.M. White, Surf. Sci. 182 (1987) 458.
[9] J. Nakamura, J.M. Campbell and C.T. Campbell, J. Chem. Soc. Faraday Trans. 86 (1990) 2725.
[10] C.T. Campbell, Adv. Catal. 36 (1989) 1.
[11] C.J. Giang, D.L. Trimm, M.S. Wainwright and N.W. Cant, Appl. Catal. 97 (1993) 145.
[12] B.A. Peppley, J.C. Amphlett, L.M. Kearns and R.F. Mann, Appl. Catal. A 179 (1999) 31.
[13] M.M. Günter, T. Ressler, R.E. Jentoft and B. Bems, J. Catal. 203 (2001) 133.
[14] T.L. Reitz, P.L. Lee, K.F. Czaplewski, J.C. Lang, K.E. Popp and H.H. Kung, J. Catal. 199 (2001) 193.
[15] PDF # 41-0254, JCPDS Powder Diffraction File, Int. Center for Diffraction Data, Swarthmore, PA, 1989.
[16] PDF # 33-0480, JCPDS Powder Diffraction File, Int. Center for Diffraction Data, Swarthmore, PA, 1989.
[17] PDF # 05-0667, JCPDS Powder Diffraction File, Int. Center for Diffraction Data, Swarthmore, PA, 1989.
[18] W.-P. Dow, Y.-P. Wang and T.J. Huang, J. Catal. 160 (1996) 155.
[19] W.-P. Dow and T.J. Huang, Appl. Catal. A 141 (1996) 17.
[20] M. Fernández-García, I. Rodríguez-Ramos, P. Ferreira-Aparicio and A. Guerro-Ruiz, J. Catal. 178 (1998) 253.
[21] M.K. Neylon, C. Marshall and J. Kropf, to be published.
[22] M.S.W. Vong, P.A. Sermon and K. Grant, Catal. Lett. 4 (1990) 15.
[23] P. Norby and J. Hanson, Catal. Today, 39 (1998) 301; and references therein.
[24] T. Ressler, R.E. Jentoft, J. Wienold, M.M. Günter and O. Timpe, J. Phys. Chem. B 104 (2000) 6360.
[25] J.A. Rodriguez, J.C. Hanson, A. Frenkel, J.-Y. Kim and M. Perez, J. Am. Chem. Soc. 124 (2002) 346.
[26] S. Poulston, P.M. Parlett, P. Stone and M. Bowker, Surf. Interf. Anal. 24 (1996) 811.
[27] J.A. Rodriguez and J. Hrbek, J. Vac. Sci. Technol. A 12 (1994) 2140.
[28] J.G. Chen, Surf. Sci. Reports 30 (1997) 1.
[29] P.J. Chupas, M.F. Ciraolo, J.C. Hanson and C.P. Grey, J. Am. Chem. Soc. 123 (2001) 1694.
[30] B.S. Clausen, G. Steffensen, B. Fabius, J. Villadsen, R. Freidenhans and H. Topsoe, J. Catal. 132 (1991) 524.
[31] A.P. Hammersely, S.O. Svensson and A. Thompson, Nucl. Instrum. Methods Phys. Res. 346 (1994) 321.
[32] J.A. Rodriguez and M. Kuhn, J. Phys. Chem. 99 (1995) 9567.
[33] J.Y. Kim, J.A. Rodriguez, J.C. Hanson, A.I. Frenkel and P.L. Lee, to be published.
[34] V.E. Henrich and P.A. Cox, *The Surface Science of Oxides* (Cambridge University Press, Cambridge, UK, 1994).
[35] B. Delmon in: *Handbook of Heterogeneous Catalysis*, eds. G. Ertl, H. Knözinger and J. Weitkamp (VCH-Wiley, New York, 1997) p. 264.
[36] J.A. Rodriguez, J.-Y. Kim, J.C. Hanson and J.L. Brito, Catal. Lett. 82 (2002) 103.
[37] R.P. Furstenau, G. McDougall and M.A. Langell, Surf. Sci. 150 (1985) 55.
[38] J.G. Chen, D.A. Fischer, J. Hardenbergh and R.B. Hall, Surf. Sci. 279 (1992) 13.
[39] To be published.
[40] R.G. Herman, K. Klier, G.W. Simmons, B.P. Finn, J.B. Bulko and T.P. Kobylinski, J. Catal. 56 (1979) 407.